Available online at www.sciencedirect.com
ScienceDirect
International Journal of Heat and Mass Transfer 50 (2007) 3141–3151
International Journal of HEAT and MASS TRANSFER
www.elsevier.com/locate/ijhmt

Natural convection between two floors of a building via a horizontal opening – Measurements in a one-half scale model

M.R. Mokhtarzadeh-Dehghan

School of Engineering and Design, Brunel University, Uxbridge, Middlesex, UB8 3PH, UK

Received 10 May 2006
Available online 26 February 2007

Abstract

The paper describes the results of an experimental study of natural convection in a closed half-scale model of a building comprising two floors connected by a stairway, and a horizontal opening between the two floors. The driving force for the flow is a heat source in the lower floor. The results indicate a complex three-dimensional flow within the model. The rate of heat losses from each wall, wall temperatures, air speed and temperature in the horizontal opening for a range of heat inputs are presented and discussed. The results are then used to suggest boundary conditions for numerical simulation of the flow.

Keywords: Building; Stairwell; Natural convection; Modelling

1. Introduction

Buoyancy-driven fluid flows occur in many fields of science and engineering. In building applications, such flows are important because of their relevance to energy conservation, ventilation and transfer of energy and mass between different zones [1,2]. The air movement within a building has a complex and three-dimensional nature, normally driven by a combination of natural and forced convection. The former mode is provided by buoyancy forces.

Numerous experimental and theoretical investigations have been carried out to gain a better understanding of natural convection flows. A review of previous work is provided by Linden [1]. Among other recent studies are those of Ziskind et al. [3] and Awbi and Hatton [4–6]. Ziskind et al. [3] reported the results of an experimental and numerical investigation of natural convection flow in a scaled model of a one-storey building and also numerical simulations of a full-scale model. The geometry comprised of a quadrilateral room with two horizontal openings located on the upper surface (roof) of the room, one acting as the inlet and the other as the outlet. The heat source, simulating an element heated by solar radiation, was a heated plate, which was also located in the same plane. The results showed that ventilation by natural convection can be achieved by such heating arrangement. Extensive experimental studies of convective heat transfer coefficient for the internal surfaces of a room using an environmental chamber were carried out by Awbi [4] and Awbi and Hatton [5,6]. They calculated convective heat transfer coefficients for the horizontal and vertical surfaces of a room with natural convection induced by heating the wall tested [4,5]. They also obtained convective heat transfer coefficient for mixed convection flows, set with the aid of a fan placed within the room [6]. In the study reported by Awbi [4], simulations using CFD were also conducted and the results were compared. This study was concerned with assessing the value of heat transfer coefficient obtained using CFD. The results showed sensitivity of the values to the near wall models and grid distribution near the wall. The measurements reported by Awbi and Hatton [5,6] provided extensive data for heat transfer coefficient and comparisons with existing data in the literature.

A less researched field of study is buoyancy-driven flow between floors of a building via stairwells, in which the

E-mail address: reza.mokhtarzadeh@brunel.ac.uk

0017-9310/$ - see front matter © 2007 Elsevier Ltd. All rights reserved.
doi:10.1016/j.ijheatmasstransfer.2006.12.002

Nomenclature

A	area of horizontal opening [m^2]	T	air temperature in horizontal opening [°C]
c_p	specific heat at constant pressure [kJ/kg K]	T_a	ambient air
g	gravitational acceleration [m/s^2]	T_{av}	average temperature in horizontal opening
h	height of the model [m]	T_i	average inside wall temperature [°C]
Q	total nominal heat input [W]	T_o	average outside wall temperature [°C]
Q_{in}	measured total heat loss [W]	T_w	average wall temperature [°C]
Q_c	local heat loss [W]	V	velocity magnitude in horizontal opening [m/s]
Q_f	wall heat flux [W/m^2]	X_1	distance along the length of horizontal opening [m]
Q_l	heat loss from a wall [W]		
Re	Reynolds number, $Re = VA^{0.5}/v$	v	kinematic viscosity [m^2/s]
St	Stanton number, $St = Q/\rho c_p T_{av} A(gh)^{0.5}$	ρ	density [kg/m^3]

work presented in this paper falls. The present author and co-investigators [7–11] carried out a series of experimental and numerical studies of buoyancy-driven flows using a half-scale two-storey building model with the main aim of obtaining a better understanding of the transfer of mass and energy between the two floors via the connecting stairwell. These studies also provide references for the previous work of other investigators. In these studies, the stairwell was the main component of the model. The driving force for the buoyancy-driven flow was a heat source placed in the lower floor of the model. The air rising from the region of the heat source passed through the stairwell, entered the upper floor and then recirculated back to the lower floor. The design features of this stairwell model resulted in an air flow which was predominantly two-dimensional. In spite of the simplicity of the model compared with a real building, some basic understanding of the flows was obtained.

The work presented in this paper resulted from a need to study the flow in a more realistic model. For this purpose the experimental model, which will be described later in this paper, was constructed. In comparison with the previous model, the present model has the three main components: the lower floor (or compartment), stairwell and the upper floor. The heat source is also placed in a more realistic position on the lower floor and the resulting flow is fully three-dimensional, more representative of complex flows which occur in buildings. Recently, Ergin [12] provided further analysis of the experimental data obtained in the previous studies [7,8] focussing on the effect of radiation exchange between the surfaces of the stairwell model. Peppes et al. [13] carried out measurements in a two-floor residential building. They studied the buoyancy-driven flows between the two floors through a single stairwell, with a horizontal opening at the junction with the upper floor. The experimental method used a single tracer gas decay technique, sensors to measure air temperatures, and infrared thermometers to measure wall surface temperatures. Peppes et al. derived empirical relationships for the rate of heat and mass transfer through the horizontal opening in terms of the average temperature difference between the two zones. This study also involved a transient three-dimensional numerical modelling of the flow, which highlighted the existence of complex flow characteristics including strong three-dimensionality and vortical motions. Further measurements and CFD simulations were reported by Peppes et al. [14] who studied the flow in another three-storey residential building. These results confirmed the findings of the earlier study. Qin et al. [15] adopted a large eddy simulation in order to study the fire induced flow of air and the combustion product (CO_2) through a three-storey building model with two stairwell shafts. The model had two openings (doors), one was placed in the same floor as the fire and the other was located at the top floor. With the lower door closed, the results showed the formation of a distinct layer of smoke with higher temperature moving upwards above a layer of air with lower temperature moving downwards. The downward flow of air was due to the open door at the top floor. In another type of experiment, while the upper door was kept open, the lower door was opened gradually. The results showed that, as the door opened, the width of the smoke flow increased, whereas the width of the airflow decreased, such that for a certain percentage opening of the lower door, smoke occupied the whole stairwell. Their partial validation of the large eddy simulation computer code was achieved by simulating the experimental conditions of Ergin-Özkan et al. [10] for non-combusting buoyancy-driven flow in a stairwell model.

The above studies show increasing interest in a better understanding of buoyancy-driven flows in stairwells. The contribution of the present work is in providing new experimental data for a complex three-dimensional natural convection flow in a new experimental setting. The presented data can also be used as a basis for further study of the flow by numerical simulation.

2. Experimental model

Fig. 1 shows the physical characteristics of the model whose overall internal dimensions are $3460 \times 1220 \times 2386$ mm ($L \times W \times H$). Other dimensions of the model and the definition of walls are given in Tables 1 and 2,

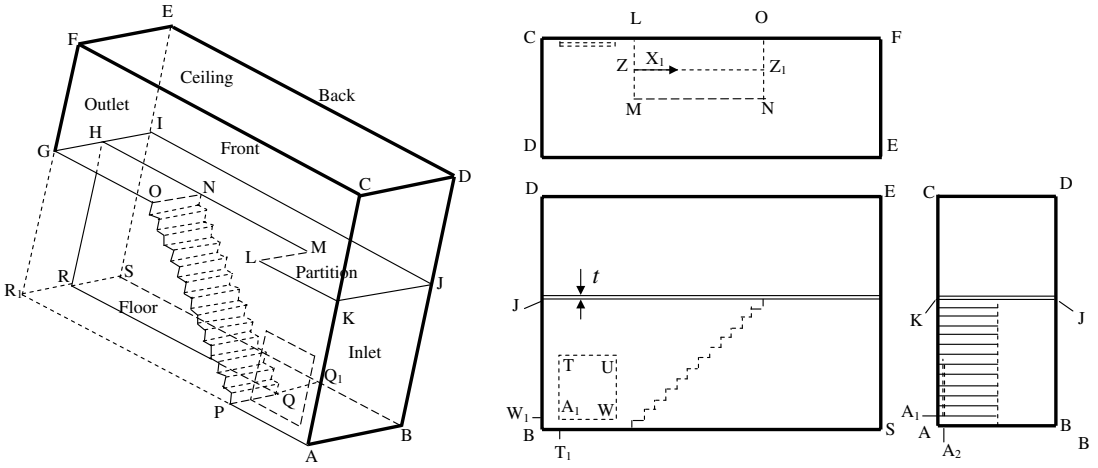

Fig. 1. Schematic diagram of experimental rig.

Table 1
Dimensions of the walls (mm)

AB	1220	RS, HI	612
AC	2386	TU	580
BS	3460	UW	650
AK, BJ	1344	AA_1, BW_1	100
AP, KL	940	BT_1	180
PQ, LM	608	AA_2	50
MN, LO	1320	t	18
OG	1200		

Table 2
Definition of the walls

AKLP	Front lower 1	$QRSQ_1$	Floor 2
PLO	Front lower 2	$PQRR_1$	Floor 3
$POGR_1$	Front lower 3	AKJB	Inlet lower
KGFC	Front upper	KCDJ	Inlet upper
BSIJ	Back lower	RHIS	Outlet lower 1
JIED	Back upper	$RHGR_1$	Outlet lower 2
CFED	Ceiling	GFEI	Outlet upper
APQ_1B	Floor 1		

respectively. The model consists of a lower compartment and an upper compartment, separated by a partition, and a thirteen step staircase. There is a horizontal opening at the top of the staircase in the plane of the partition and measures 1320×608 mm. The space under the stairs is blocked off from the inside and outside of the model, thus there is no air exchange between this space and the internal space of the model or the external environment. There are also no connections from the inside of the model to the external environment through openings; the model forms a closed system.

The floor of the model, the two end walls (referred to as the inlet and outlet walls), the ceiling and the partition are constructed from large single sheets of 18 mm thick blockboard. The front and the back walls are constructed from smaller 10 mm transparent acrylic (Perspex) sheets. The steps of the staircase are constructed from 4 mm plywood mounted on an 18 mm blockboard base. The model rests on a Dexion steel frame. The floor of the model is at a distance of 0.30 m from the laboratory floor. The wooden and acrylic panels are joined by screws, and self-adhesive tape is placed on the joints to prevent air leakage. All internal surfaces (except the front and rear acrylic walls) are painted black. The total mass of the building model is approximately 450 kg.

The heat source is a 1 kW oil-filled panel heater with overall dimensions 650×580 mm ($H \times W$). It has a corrugated surface with a round base. The main vertical surface area has an average thickness of 25 mm. The heater was located longitudinally at the base of the staircase 50 mm away from the front wall and 180 mm from the inlet wall. Its base was at a distance of 100 mm from the floor. The heat input was controlled using a Variac and was measured by a digital wattmeter. The results reported here are for four nominal heat inputs, namely 300, 450, 600 and 750 W. A metallic sheet slightly larger than the radiator was attached to the front wall in front of the heater to prevent heat damaging the acrylic.

The model was placed in a laboratory with the internal dimensions $8.9 \times 4.3 \times 3.2$ m ($L \times W \times H$). Apart from a double-width entrance door, there were no other openings into the laboratory. The gap between the door and the floor was covered. This arrangement minimised the effects of draught.

The following measurements were carried out: the internal and external wall surface temperatures over defined grids, heat input from the heater, air temperature and velocity along a straight line in the middle of the horizontal opening (Z–Z1 in Fig. 1). The measurement grids divided the internal and external surfaces of the walls of the model into smaller areas (cells). The front and rear walls each consisted of 20 grid cells. The floor had 17, the ceiling, 15, the inlet wall, 15, and the outlet wall, 14. Therefore, a total of 101 thermocouples were used on the internal surfaces and the same number on the external surfaces. They were attached at the centre of each grid cell. The temperatures measured at these points were used to calculate the

heat losses through the walls. For the measurement of air velocity and temperature in the horizontal opening, a one-dimensional grid in the mid-section of the horizontal opening was used, consisting of 10 points. Each of these measurement stations consisted of a 20 mm diameter hole drilled in the front wall, through which the probes were inserted. Careful attention was paid to minimize air leakage through the joints between the walls of the model. Leakage tests were carried out to determine the degree of air tightness of the model. For this purpose, a concentration decay method was used, utilizing an infrared gas analyser with carbon dioxide as the tracer gas. These tests showed that the leakage rate through the joints of the model was negligible.

3. Instrumentation

The main instruments were thermocouples, nine platinum resistance thermometers to measure air temperature and one air velocity transducer.

The thermocouples were type K, Ni–Cr/Ni–Al with an operating range from 0 to 250 °C. The thermocouple extension leads were 3 m long and were insulated. The thermocouples were wired to 20 multi-switch units whose voltage signals were input to a digital microprocessor thermometer. Consideration for the overall achieved heat balance given below indicates that the accuracy of measured temperature differences could be taken as ±0.05 °C, although the uncertainty in the individual temperatures is higher, about ±0.1 °C.

The thermocouples were attached to the wall surfaces as follows. For internal attachment, the thermocouple lead was inserted through a 1 mm diameter hole drilled in the wall such that its measuring junction was flush with the internal wall surface. A strip of adhesive tape was used on the external surface of the wall to hold the thermocouple wire firmly in its place and to prevent any air leakage through the hole. For external attachment, the thermocouples were fixed to the wall surfaces using a strip of self-adhesive tape. The most suitable method to measure wall surface temperature depends on the specific situation. The method adapted in these experiments was considered to be suitable because of relatively small temperature gradients present and a very long period of time allowed for stabilisation of temperatures, so that the very small thermocouple junction and the local surroundings reach the same temperature.

The air temperature in the opening was measured using platinum resistance thermometers. The output from the probe was linear from 0 to 100 mV for temperatures in the range of 0–100 °C. The time constant was 3 min and the accuracy of measurements was within ±0.05 °C.

The instrument for air velocity measurement was a TSI velocity transducer model 7470 constant temperature thermal anemometer, with temperature compensation in the range of 7–60 °C, an operating range of 0.05–1.0 m s^{-1} and a time constant of 2 s. It had a spherical sensor of 3 mm diameter and thus measured the velocity magnitude. The velocity transducer was calibrated to provide a linear output between 0 and 5 V for 0–1.0 m s^{-1}. The accuracy of the measurements using this probe was within ±5%.

The working length of the probe was 450 mm. The air velocities and temperatures were collected using a data acquisition system, which comprised a computer, an IEEE interface card and two digital-to-analogue converters. Forty readings of air velocity and one reading of air temperature at each measurement station were taken and the sequence was repeated five times. This process took about 3 min, at the end of which the averaged values of the readings were recorded.

4. Experimental methodology

Prior to experiments, the following procedures were followed. The heat input was set to the desired value. All the lights were turned off except a 40 W desktop lamp placed far from the model. The only door to the laboratory was shut and the model was left alone for at least two days during which occasional inspections of the experimental conditions were carried out. During the measurement period, air temperature and velocity were measured by the data logging system at least eight times. The wall temperature readings were very stable with maximum changes of ±0.1 °C. This sequence of measurements was then repeated once more. Subsequently, the laboratory was left alone for at least 4–5 h before another set of readings were taken. The results from different tests were consistent and repeatable. For new tests with new heat input, the time period for stabilization of the experimental conditions was at least two days.

4.1. Processing of the data

Heat losses through the walls of the building model were calculated using the thermal conductivities of the wall materials, thicknesses of the walls and the measured temperature differences between the internal and external surfaces of the walls. The thermal conductivities of blockboard and acrylic were taken as 0.14 and 0.19 W m^{-1} K^{-1}, respectively. It was mentioned previously that there was a total of 101 temperature measurement locations on the walls. Therefore, the heat loss calculations were carried out using the same number of grid cells. These calculations were based on the assumption that the wall temperature remained constant over the cell area.

Table 3 shows the values of heat loss from the walls of the model. For the inlet, outlet, front and back walls, the total heat loss is broken down into the losses associated with the upper compartment and lower compartment. The results shown in Table 3 were obtained from averaging the results of a number of tests. For 300 W nominal heat input, it can be seen that the total heat loss obtained by measurement is 275.2 W, which is lower than the measured average heat input of 299 W by about 8%. For nominal

Table 3
Heat loss from stairwell walls at different heat inputs

	Q_{in} [w]	299	454	597	751	Area [m^2]
		Q_l [W]				
Inlet	Lower wall	29.6	43.2	57.3	72.1	1.68
	Upper wall	7.7	12.7	17.3	22.4	1.3
	Total loss	37.3	55.9	74.6	94.5	2.98
	% of Q_{in}	12.5	12.3	12.5	12.6	
Outlet	Lower wall 1	7.4	11.8	15.3	19.5	0.86
	(Lower wall 2)	0.5	1.9	2.5	3.8	0.82
	Upper wall	8.2	12.3	16.2	21.3	1.3
	Total loss	16.1	26.0	34.0	44.6	2.98
	% of Q_{in}	5.4	5.7	5.7	5.9	
Back	Lower wall	60.8	96.2	126.9	159.8	4.73
	Upper wall	28.9	44.3	55.7	72.0	3.67
	Total loss	89.7	140.5	182.6	231.8	8.43
	% of Q_{in}	30.0	31.0	30.6	30.9	
Front	Lower 1	34.5	51.6	73.4	90.3	1.3
	Lower 2	9.4	15.3	21.0	25.5	0.89
	(Lower 3)	0.0	0.24	3.7	6.6	2.54
	Upper wall	21.9	41.5	53.2	70.4	3.67
	Total loss	65.8	108.6	151.3	192.8	8.43
	% of Q_{in}	22.0	23.9	25.3	25.7	
Floor	Floor 1	23.8	35.3	43.9	52.6	1.19
	Floor 2	15.5	18.4	22.1	25.8	1.6
	(Floor 3)	6.9	7.1	7.3	7.6	1.54
	Total Floor	46.2	60.8	73.3	86.0	4.33
	% of Q_{in}	15.4	13.4	12.3	11.5	
Ceiling	Ceiling	20.2	37.4	54.7	76.8	4.33
	% of Q_{in}	6.8	8.2	9.2	10.22	
	Total [W]	275.2	431.8	571.7	726.4	
	% Q	92.2	94.6	95.5	96.7	
	% from upper	31.5	34.5	34.5	36.2	
	T_a [°C]	23.8	22.2	25.3	24.6	

The areas shown within brackets relate to the space below the stairway which is blocked off.

heat inputs of 450, 600 and 750 W, the percentage difference is smaller, between 3% and 5%. The exact heat balance is not expected because the calculation of heat loss depends on a number of contributing factors. As was referred to above, it was assumed that the wall temperature was uniform over the cell area. The leakage is taken to be negligible but the heat losses through the temperature probe supports, used in the measurement of air temperature, and losses by thermal radiation through the Perspex walls are unaccounted for. The calculation of heat loss also involves a number of uncertainties, because its value is a function of wall thickness, thermal heat conductivity and temperature difference. The wall thickness may differ from the nominal value by ±0.5 mm. A sensitivity analysis showed that changing the thickness of the wooden walls by ±0.5 mm, while other parameters kept constant, resulted in changes in the total heat loss within ±1.2%, whereas such changes for the thickness of the Perspex walls resulted in changes within ±3%. There is also a degree of uncertainty in the values of heat conductivity for wood and acrylic. Again, a sensitivity analysis was carried out by changing the values by ±0.01 W m^{-1} K^{-1}. Such changes in the wood and Perspex conductivities resulted in changes of the total heat loss by about ±3. Lastly, a sensitivity analysis was carried out to assess the significance of ±0.05 °C uncertainty in temperature difference. For this purpose the average temperature difference over each wall was used. It was found that the changes in the total heat flux from each wall for 300, 450, 600 and 750 W heat inputs were in the range of 3–9%, 2–6%, 2–5% and 1–4%, respectively, and for the total heat flux from the model were 7%, 5%, 4% and 3%, respectively. A greater percentage of error in temperature difference of say ±0.1 °C, would result in much greater deviations of the measured total heat input from the total heat output referred to above, beyond a level which could be explained.

5. Results and discussion

Fig. 2 shows the local percentage heat loss from various cells on each wall of the model for the nominal heat inputs of 300, 450, 600 W and 750 W. The average values are also shown in Fig. 2. Another representation of the sensitivity of heat loss to heat input can be seen in Fig. 3, where the variations of the total percentage heat loss from each wall are shown. The results for the back, inlet and outlet walls (Fig. 2b–d) show the least sensitivity to the heat input, whereas the results for the front wall, floor and the ceiling (Fig. 2a, e, and f) show much greater sensitivity. The low sensitivity of percentage heat loss to heat input suggests that an average, representative, value for each wall may be calculated. This value may be taken to be valid for heat inputs from 300 to 750 W.

The variations of heat flux as a function of heat input is shown in Fig. 4. These results indicate linear relationships between the heat flux and the heat input. They also show that, except for the outlet wall, the heat flux is greater for the walls located in the lower compartment, with the inlet showing the greatest difference between the two. For the four heat inputs, the heat loss from the upper compartment is 32%, 35%, 35% and 36% of the total measured heat input, respectively. The internal and external wall temperatures averaged over each wall are shown in Fig. 5, which also show an increase (with a decreasing rate) with heat input.

The distributions of percentage heat loss area over the walls for 300 W heat input are shown in Fig. 6. The results for other heat inputs were similar and are not included in this paper. These results help in deducing the flow path within the model. In discussing the results for each wall, in order to aid the reader to locate the position, which is being referred to, the actual value of the percentage heat loss as appears in Fig. 6 is given in brackets. Note also that the value noted may be a typical value in the region, given as an example.

Inlet (Fig. 6a). For the inlet wall, the largest heat loss (1.72) takes place from the lower part of the wall, which is closer to the heater. Above this area, the heat loss is first

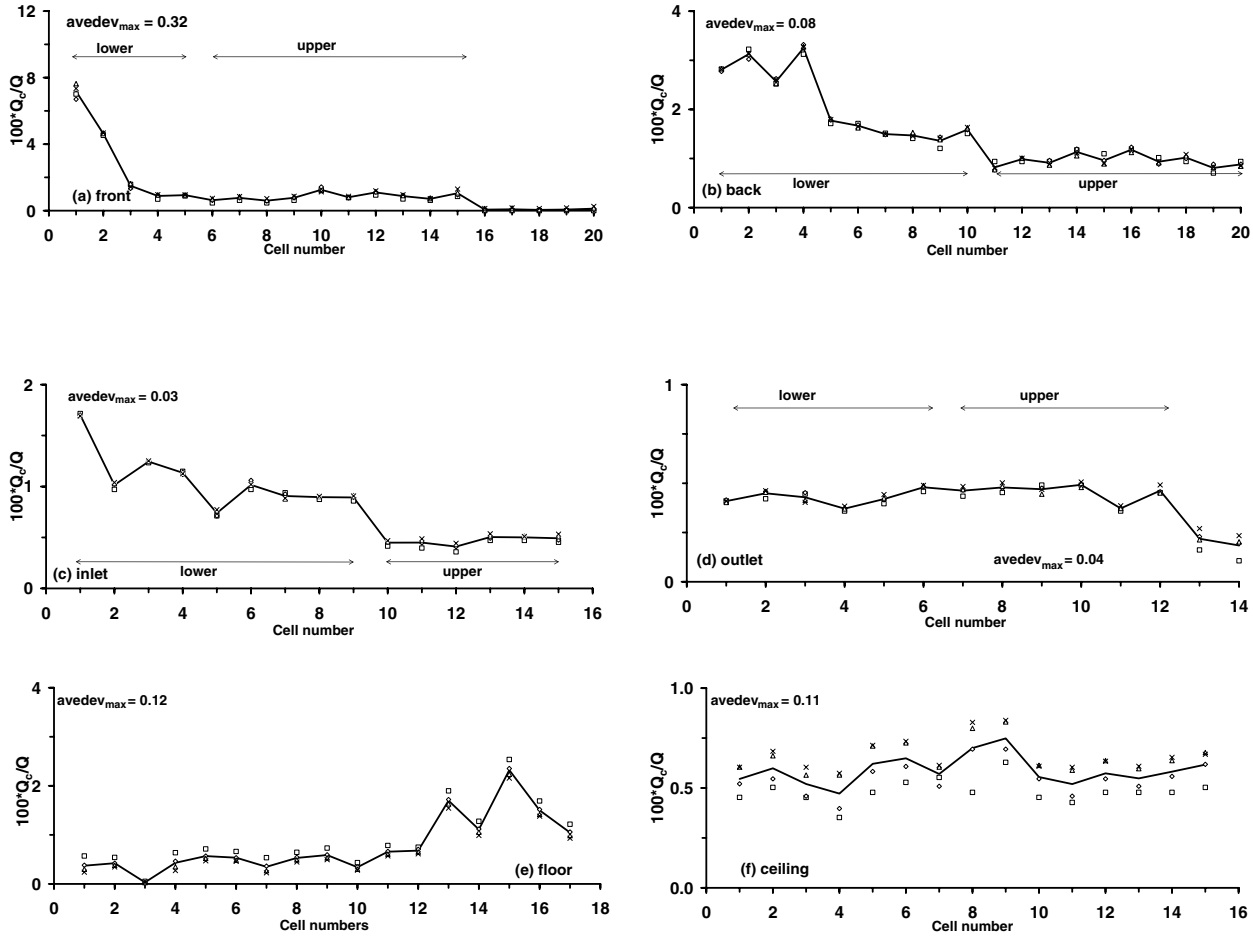

Fig. 2. Percentage heat loss from stairwell walls for different heat inputs □ 300 W, ◇ 450 W, Δ 600 W, × 750 W, — average value Avedev$_{max}$ is the maximum of average deviations from mean value.

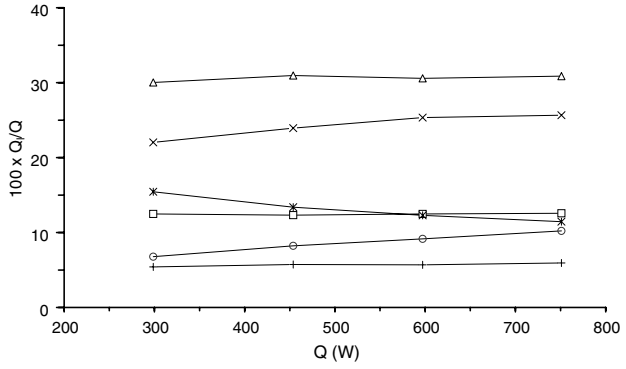

Fig. 3. Variation of percentage heat loss from the walls at different heat inputs × front, Δ back, □ inlet, + outlet, ○ ceiling, ∗ floor.

reduced (0.97) and then increased again (1.23). This is due to the flow of hot air, which rises from the region of the heater, slowed down as it approaches the partition and is then diverted to flow along the partition. The heat loss is also high (e.g. 0.87) in the region of the back wall, because of the recirculating air in the lower compartment. The heat loss from the upper part of the inlet wall located in the upper compartment is generally lower (e.g. 0.47) and is more uniform.

Outlet wall (Fig. 6b). Higher heat losses again take place from the lower part of the wall, which is adjacent to the lower compartment (e.g. 0.41) and the distribution is more uniform compared to the inlet wall. Slightly greater heat loss from the areas below the partition (e.g. 0.46) indicates the accumulation of hot air there. The upper part of the outlet wall in the upper compartment again shows more uniform distribution (e.g. 0.45) and the values are about the same magnitude as on the inlet wall. The area under the stairs shows very small heat loss.

Front wall (Fig. 6c). As expected, a high heat loss (e.g. 7.0) takes place from the area of the wall, which is opposite to the heater. There is then a sharp drop to the values (0.88) in the stairway area and further drop to values in the upper compartment. The greater values of heat loss in the stairway compared with the upper compartment is due to the hot rising air flowing from the lower to the upper compartment. The rising air is diverted by the ceiling and moves in different directions, partly towards the inlet wall, partly towards the outlet wall and partly towards the back wall, giving rise to greater heat loss from the upper part of the

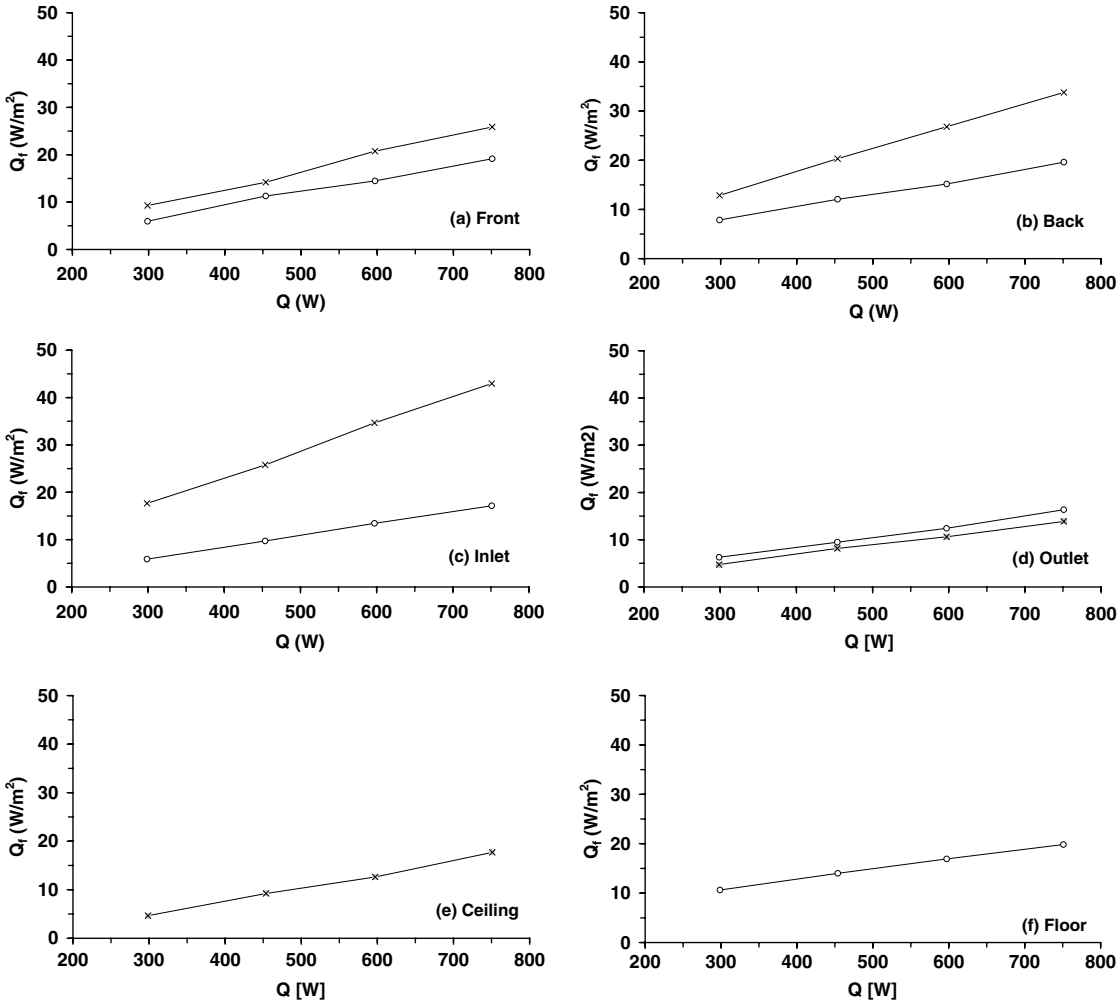

Fig. 4. Heat flux from the lower and upper walls ○ wall in upper floor, × wall in lower floor.

wall close to the ceiling (e.g. 0.62 and 0.70). The results indicate greater losses in the region close to the inlet wall (0.86) compared with the region close to the outlet wall (0.62). The air is then diverted downwards by the inlet and outlet walls and flows towards the partition, and gives rise to lower heat loss in the area close to the partition (e.g. 0.47 at outlet side and 0.62 at inlet side).

Back wall (Fig. 6d). A greater heat loss (e.g. 2.82) takes place in the lower compartment opposite to the heater. This is as a result of hot air, which rises from the heater, being partly diverted by the partition and moves towards the back wall. The heat loss from the extreme end of the back wall, near the outlet, is generally low (e.g. 1.51). In this area only very slow movement of the air is expected. The heat loss in the region of the back wall located in the upper compartment is again lower, but has relatively greater values in the mid-region and near the ceiling (1.17).

Floor (Fig. 6e). As expected, the heat loss in the region close to the heater is high (e.g. 1.90). Due to the recirculation of hot air in the lower compartment and diversion towards the back wall, the heat loss is also high (1.22) on the back wall side of the floor. Over the remaining floor area, except under the stairs, the heat loss is lower and variations are small.

Ceiling (Fig. 6f). The heat loss from the ceiling is more uniform than other walls, with only small rise (0.63) in the mid-section on the front wall side, which is the area directly above the horizontal opening, through which hot plume of air rises.

5.1. Temperature and velocity of air in the opening

Fig. 7 shows the profile of air temperature along the mid-section of the horizontal opening. Fig. 8 shows the corresponding velocity magnitude. Due to the three-dimensional nature of the flow, air temperature and velocity vary significantly in this plane. The upflow takes place mainly through part of the opening area, which is on the heater side. The downflow is mainly through the area on the stairs side. Fig. 8 shows that in the region of the upflow, the velocity magnitude increases to a peak value. Due to the diversion of the rising air from the heater, by the horizontal partition, the velocity has a large horizontal component at the start of the opening and the higher velocities, including

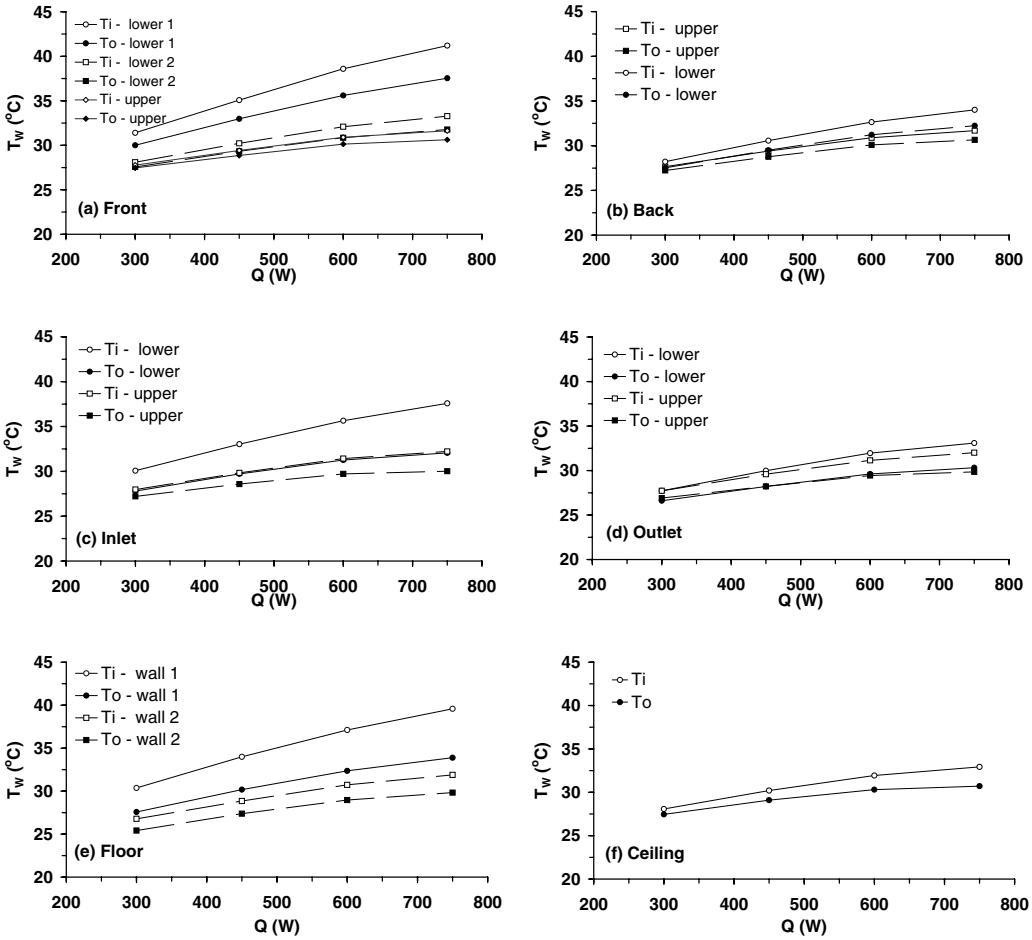

Fig. 5. Average wall temperatures T_i – inside, T_o – outside.

the peak value in Fig. 8, fall in this approximately horizontal flow. Figs. 7 and 8 show that the temperature and velocity in this region start from lower values at the start of the opening, where mixing of two air streams takes place: one is the faster and hotter air from the lower compartment and the other is the colder and slower air returning from the upper compartment. The mid-section of the horizontal opening involves rising of a hot plume of air which has generally lower velocities, but higher temperatures as seen by the peak in the temperature profile of Fig. 7. The downflow has generally lowest velocities measured and the trough in the profile of Fig. 8 is associated with this flow. It is difficult to determine exactly the position of the interface between the upflow and the downflow, because of the three-dimensional nature of the flow and generally low velocities involved. However, from the location of the peak in temperature (Fig. 7) and the location of the trough (Fig. 8), it can be concluded that the interface between the upflow and downflow is in the region between $x = 0.9$ and 1.0 m. It should be noted that there must be a mass balance between the upflow and downflow in the plane of the opening, but this cannot be satisfied by simple integration of the velocity profile in Fig. 8. This is, first because the vertical component of the velocity is not known, and secondly mass exchange between the two compartments can also take place elsewhere in the opening around the edges in a more complex way than that may be deduced from the velocity profile in Fig. 8.

Figs. 7 and 8 also show the effects of heat input on air velocity and temperature at the mid-section of the opening, which confirms the expectation that both the velocity and temperature increase with heat input. The shapes of the profiles remain the same for different heat inputs. However, the temperature profiles show that the rate of increase in temperature slows down as the heat input increases, especially from 600 to 750 W. Table 3 shows that the percentage heat loss from the upper and lower compartments is nearly independent of heat input. Therefore, slowing down of the rise in air temperature could be related to changes in the pattern of the flow in this region, causing a shift in the position of higher temperatures away from the mid-plane where the profiles were measured. In other words, the highest velocities and temperatures do not necessarily occur in the mid-plane.

Referring back to Figs. 2e and 3 indicate that the heat loss from the floor decreases with heat input, whereas the opposite effect can be seen for the ceiling (Fig. 2f). These results indicate that as the heat input increases the heated

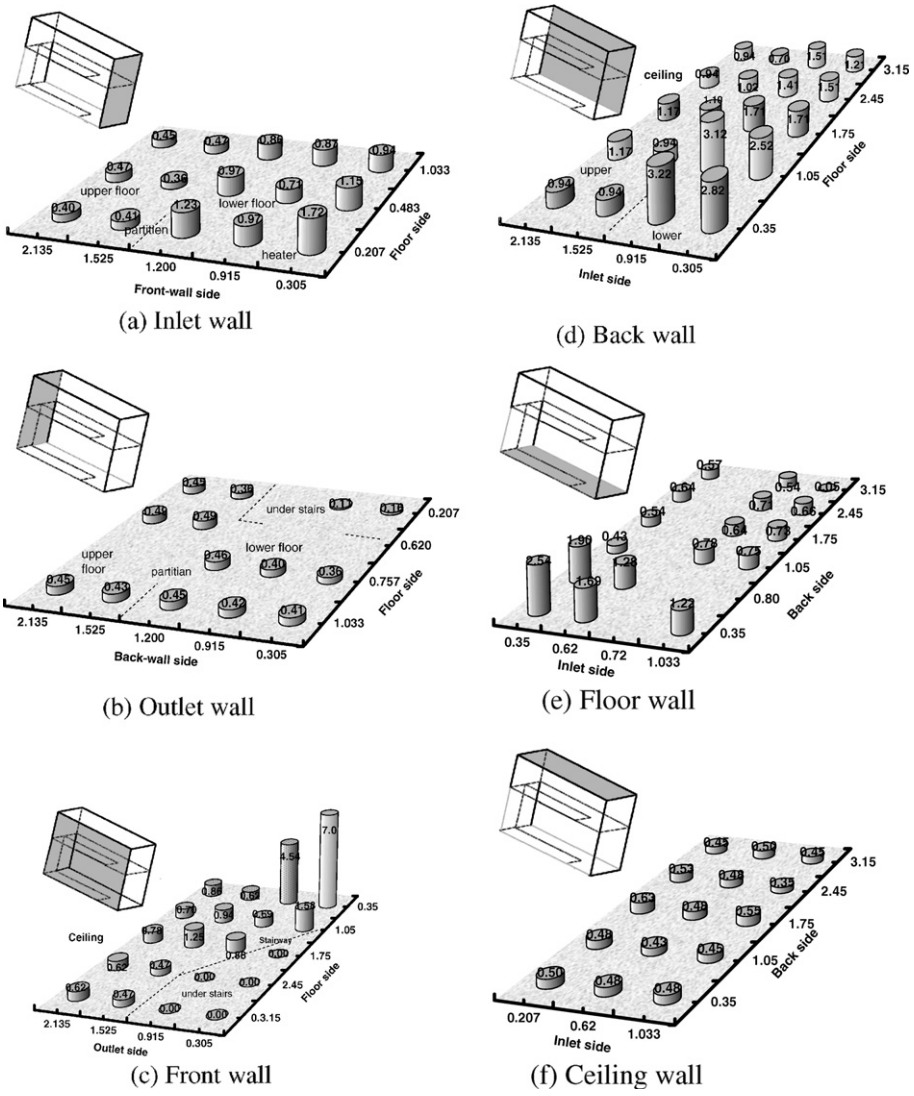

Fig. 6. Percentage heat loss ($Q_c \times 100/Q$) from stairwell walls at 300 W heat input. The axes have units of m.

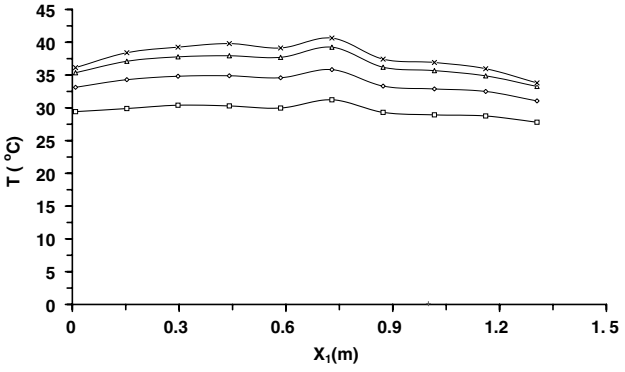

Fig. 7. Air temperature in the mid-section of the horizontal opening.

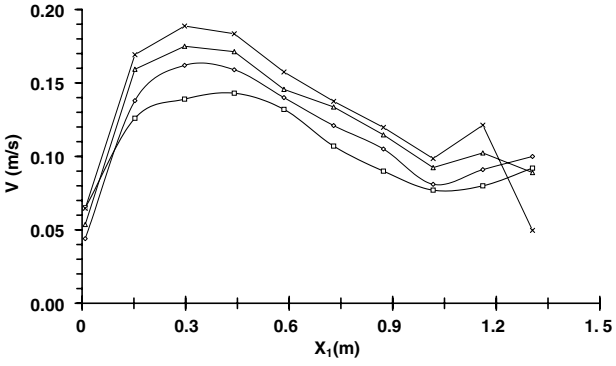

Fig. 8. Air velocity in the mid-section of the horizontal opening.

air with higher temperature is lifted away from the floor region and tends to accumulate near the ceiling with the effect of increasing the heat loss. The colder air, partly returning from the upper compartment and partly after recirculation in the lower compartment replaces the displaced hot air.

Table 4 shows the values of the dimensionless parameters Reynolds, Grashof and Stanton numbers based on

Table 4
Characteristic dimensionless numbers

	300 W	450 W	600 W	750 W
Re	5997	6511	7058	7363
St	3.09E − 04	4.64E − 04	6.19E − 04	7.73E − 04
Gr	2.01E + 08	2.77E + 08	3.29E + 08	3.68E + 08

the air velocity and temperature shown in Figs. 7 and 8 and the dimensions of the horizontal opening. For Grashof number, approximate temperature difference between the upflow and downflow is used. For Stanton number representative average temperature and for Reynolds number representative value of velocity are used. The values given in Table 4 are consistent with the values reported earlier [10] for a one-half scale stairwell model. From Table 4, the value of Gr/Re^2 which signifies the strength of buoyancy to inertia forces range from 5.5 to 7. Considering the range of velocities measured in the opening (Fig. 8), suggests that while the flow regime in most parts of the stairwell is of viscosity dominated nature, transitional to inertia dominated flow conditions exist in the horizontal opening and in the vicinity of the heater.

The previous experimental studies of the author and co-investigators [7–10] were formed the basis for parallel numerical simulations [8,9,11]. These studies provided further understanding of natural convection flows in buildings, but also were used to assess the performance of the mathematical models incorporated in computer codes. Conducting these simulations indicated that prediction of complex three-dimensional flows of the type studied is challenging and may results in inaccurate flow fields. Further comments are therefore put forward below in relation to the use of the present results for possible future numerical simulation.

In general, for fluid flow problems involving heat transfer the definition of the thermal boundary conditions is a source of uncertainty, because these are not usually known. The two main types of thermal boundary conditions are wall temperature, and wall heat flux boundary conditions. In a practical situation, in the absence of data obtained by direct measurement, the boundary conditions are approximated, or obtained by some engineering calculations, which also contain uncertainties.

In situations such as the present study, where both heat flux and wall temperatures are measured, either of them can be used as the boundary conditions. Even though, in this situation, there are possible complications. Firstly, for practical reasons, the wall temperature or heat flux may have to be taken as constant over the wall. Secondly, if the wall temperature is set as the boundary condition, then the heat flux through the wall is calculated. In this case, although in the final converged solution the overall heat balance is satisfied, the local heat flux may differ from the measured values. On the other hand, if the heat flux is set, the wall temperature is then calculated as part of the solution. In this case, although the overall heat flux is satisfied and local heat losses are in accordance with measurements, the wall temperatures may differ from the measured ones. This is because the calculation of both heat flux and temperature depends on the accuracy of the predicted flow field, and on the accuracy of the near wall models, which is part of the mathematical model.

Here before the boundary conditions are suggested, some simplifying assumptions have to be made. Firstly, the wall temperature and wall heat flux vary on all walls and a decision should be made with regard to the division of a particular wall into smaller areas such that over these areas the wall temperature or heat flux may be assumed to be constant. In the present study, the walls were already divided into smaller cells for the purpose of measurements, so these cells could be used for boundary conditions. However, setting of boundary conditions over 138 cells is rather a lengthy task. It is therefore suggested that, as first approximation, the front is divided into three cells, whereas the inlet, outlet, floor and the back wall are divided into two cells as shown in Fig. 1. The more uniform temperature distribution on the ceiling allows for the definition of one cell for this wall. The specification of the heat flux boundary conditions are therefore as already given in Table 3. Fig. 5 allows shows the setting of the temperature boundary conditions.

Further simplifications of the model relate to the space under the stairway, which is blocked off and is not included in the flow simulation. Since the heat loss from this space is small, the heat losses through the relevant walls (front lower 3, outlet lower 2 and floor 3) may be set to zero. It was noted above that the measured total heat loss was lower than the measured total heat input. If it is assumed that the deficit in heat output did not take part in the setting of the flow distribution, then the total heat input on the heater as the boundary condition can be set to be equal to the value obtained by summing the heat losses, and thus the overall heat balance is satisfied. Other simplifications relate to the partition and the geometrical representation of the heat source. In the experiments, heat transfer takes place through the partition wall because of temperature difference between the lower and upper compartments. In a more advanced simulation, this wall may be defined as internal wall and the problem as a conjugate heat transfer, so that the heat transfer through the wall is calculated as part of the solution. Otherwise, for a simpler simulation, the heat flux may be set to zero. The heat source is suggested to be modelled as a rectangular box of dimensions given in Fig. 1 with constant heat flux set on the surfaces.

6. Conclusions

A highly three-dimensional natural convection flow was induced in a half-scale model of a two-storey building by placing a heat source in the lower compartment of the model. For the range of 300–750 W heat input from the heat source, the average wall heat flux increased linearly with heat input for all the walls. However, the variations

of percentage heat loss were small, especially for the vertical walls. The horizontal walls, namely the floor and ceiling showed more sensitivity to heat input, with the ceiling showing an increase of heat loss, whereas the floor showing the opposite effect. The total heat loss from the upper compartment was in the range of 32–36% of the heat input. The average inside and outside wall temperatures also increased with heat input, but showed a small non-linearity. The deduced flow pattern indicated the existence of a number of large three-dimensional recirculating flow regions. The interaction between the upflow and downflow took place in the region of the horizontal opening. In this region, the measured velocity showed greater values in the upflow compared with the downflow. The results also pointed to a complex three-dimensional flow pattern in this region, with downflow possibly taking place around the edges of the opening. The velocities measured did not exceed 0.2 m/s, indicating very slow flow of laminar nature within majority of the internal volume of the model. Higher velocities and transition to turbulence are expected to take place near the heater surfaces. It would be interesting to assess the performance of current CFD models in predicting this mixed laminar and turbulent flow, especially with regard to the choice of turbulence models and near wall models, or in the application of large eddy simulation. For this reasons possible use of the results as boundary conditions was suggested.

References

[1] P.F. Linden, The fluid mechanics of natural ventilation, Ann. Rev. Fluid Mech. 31 (1999) 201–238.
[2] M. Fordham, Natural ventilation, Renew. Energ. 19 (2000) 17–37.
[3] G. Ziskind, V. Dubovsky, R. Letan, Ventilation by natural convection of a one-storey building, Energ. Build. 34 (2002) 91–102.
[4] H.B. Awbi, Calculation of convective heat transfer coefficients of room surfaces for natural convection, Energ. Build. 28 (1998) 219–227.
[5] H.B. Awbi, A. Hatton, Natural convection from heated room surfaces, Energ. Build. 30 (1999) 233–244.
[6] H.B. Awbi, A. Hatton, Mixed convection from heated room surfaces, Energ. Build. 32 (2000) 153–166.
[7] A.S. Zohrabian, M.R. Mokhtarzadeh-Dehghan, A.J. Reynolds, B.S.T. Marriot, An experimental study of buoyancy-driven flow in a half-scale stairwell model, Build. Environ. 24 (1989) 141–148.
[8] A.S. Zohrabian, An experimental and theoretical study of buoyancy-driven air flow on a half-scale stairwell model, PhD thesis, Department of Mechanical Engineering, Brunel University, 1989.
[9] S. Ergin-Özkan, Measurements and numerical modelling of natural convection in a stairwell model, PhD thesis, Department of Mechanical Engineering, Brunel University, 1993.
[10] S. Ergin-Özkan, M.R. Mokhtarzadeh-Dehghan, A.J. Reynolds, Experimental study of natural convection between two compartments of a stairwell, Int. J. Heat Mass Transfer 38 (12) (1995) 2159–2168.
[11] M.R. Mokhtarzadeh-Dehghan, S. Ergin-Özkan, A.J. Reynolds, Natural convection between two compartments of a stairwell-numerical prediction and comparison with experiment, Numer. Heat Transfer 27 (1995) 1–17.
[12] S. Ergin, Surface radiation with conduction and natural convection in a two-floor enclosure, Energ. Build. 32 (2000) 57–70.
[13] A.A. Peppes, M. Santamouris, D.N. Asimakopoulos, Buoyancy-driven flow through a stairwell, Build. Environ. 36 (2001) 167–180.
[14] A.A. Peppes, M. Santamouris, D.N. Asimakopoulos, Experimental and numerical study of buoyancy-driven stairwell flow in a three storey building, Build. Environ. 37 (2002) 497–506.
[15] T.X. Qin, Y.C. Guo, C.K. Chan, K.S. Lau, W.Y. Lin, Numerical simulation of fire-induced flow through a stairwell, Build. Environ. 40 (2005) 183–194.